Dynamic Monte Carlo simulations of the three-dimensional random-bond Potts model

J. Q. Yin,[1] B. Zheng,[1,2] and S. Trimper[2]
[1]*Zhejiang University, Zhejiang Institute of Modern Physics, Hangzhou 310027, China*
[2]*FB Physik, Universität-Halle, 06099 Halle, Germany*
(Received 1 April 2005; revised manuscript received 27 May 2005; published 23 September 2005)

The effect of random bonds on the phase transitions of the three-dimensional three-state Potts model is investigated with extensive dynamic Monte Carlo simulations. In the weakly disordered regime, the phase diagram is obtained with a recently suggested nonequilibrium reweighting method. The tricritical point separating the first- and second-order transitions is determined, and the critical exponents of the continuous phase transition induced by quenched randomness are estimated.

DOI: 10.1103/PhysRevE.72.036122 PACS number(s): 64.60.Fr, 05.50.+q, 75.40.Mg, 64.60.Ht

I. INTRODUCTION

The influence of quenched disorder on phase transitions has been the subject of substantial interest for physicists in the past years. Schwenger *et al.* [1] investigated experimentally the critical behavior of the order-disorder phase transition of the (2×2)-2H structure on Ni(111) for the pure system and in the presence of 0.3%-3% of a monolayer of preadsorbed atomic oxygen. It was found that depending on the oxygen concentration, the values of the critical exponents change from those of the four-state Potts universality class to the Ising-like exponents. This behavior is qualitatively in agreement with the effect of random quenched impurities. An extensive experimental study [2] of the isotropic to nematic phase transition of *n*CB liquid crystals in aerogel shows that the transition temperature is lowered compared to the pure case and that the transition changes from first order to a continuous one.

Earlier theoretical works [3–5] on disordered systems indicate that quenched disorder could produce rounding of a first-order phase transition and, thus, induce a second-order one. The pure Potts model exhibits a temperature-driven first- or second-order phase transition, depending on the state q and spatial dimension D. The disordered Potts model is therefore a good laboratory for the study of the effect of quenched disorder on phase transitions. In two dimensions, the critical point of the random-bond Potts model with a self-dual bimodal distribution is even known exactly [6]. This is an advantage for numerical simulations. Aizenman and Wehr [5] have rigorously proved that for $D\leqslant 2$, an *arbitrarily* weak amount of quenched bond randomness leads to elimination of any discontinuity in the density of the variable conjugate to the fluctuating parameter. Along this understanding, many activities in the last decade have been devoted to the two-dimensional random-bond Potts model [7–21].

For the random-bond Potts model in higher dimensions, theoretically it is shown that a tricritical point may appear at a finite concentration of impurities [12], and it separates the first- and second-order transitions. In three dimensions, for understanding the influence of disorder on first-order transitions, the first numerical study of the Potts models with quenched disorder was presented in Ref. [22], and recently, the site-diluted three-state and bond-diluted four-state Potts models [23,24] have been studied with Monte Carlo simulations. Numerical evidence for the existence of a tricritical point was reported. The authors of Ref. [24] also estimated the critical exponents of the induced continuous transition. It was found that the exponents $\beta/\nu=0.65(5)$ and $\nu=0.752(14)$ are clearly different from those of either the three-dimensional (3D) disordered Ising [25–27] or the three-state site-diluted Potts model. On the other hand, it is interesting and important to investigate numerically the general effect of random bonds on phase transitions and critical dynamics. However, due to strong critical slowing down induced by the bond disorder and the numerical difficulties of distinguishing second-order and weak first-order phase transitions, numerical simulations of the three-dimensional random-bond Potts model are not easy even in the case of a symmetric bimodal distribution. Recently, some effort has been made in this direction, and numerical simulations as well as analytical results are reported for the large-q-state random-bond Potts model in three dimensions [28].

In 1989, with renormalization group methods Janssen, Schaub, and Schmittmann derived a dynamic scaling form for the $O(N)$ vector model, which is valid up to the *macroscopic short-time regime*, after a microscopic time scale t_{mic} [29]. The dynamic process they considered is that the system initially at a very high temperature state with a small or zero magnetization is suddenly quenched to the critical temperature and then released to the dynamic evolution of model *A*. Such a short-time dynamic scaling behavior has been numerically verified [30–34], and it is also consistent with relevant theories and experiments in spin glasses. Furthermore, the short-time dynamic scaling can be extended to the dynamic relaxation starting from an ordered state [33,35,36].

More interestingly, based on the short-time dynamic scaling, it is possible to extract not only the dynamic exponents, but also the static exponents as well as the critical temperature [33,37–39]. Since the measurements are carried out in the short-time regime of the dynamic evolution, the method does *not* suffer from a critical slowing down. What we pay for this approach is that the measurements of the dynamic exponents and static exponents cannot be separated. Therefore, the statistical errors of the static exponents include those from the dynamic exponents. However, if we are also

interested in the dynamic behavior, the short-time dynamic approach is rather useful. Compared with the nonlocal cluster algorithms, the dynamic approach does study the dynamics local in time and, in general, applies also to disordered systems [21,40,41].

On the other hand, in the last two decades, much effort [42–46] has been devoted to the subject of reweighting techniques in Monte Carlo simulations in equilibrium. These reweighting methods have greatly improved the efficiencies of Monte Carlo simulations in many aspects. Therefore, it is rather appealing to develop a dynamic reweighting method. Such a technique for a contact process was first proposed by Dickman [47]. Recently, a rather generic reweighting method for nonequilibrium Markov processes was presented by Lee and Okabe [48]. With nonequilibrium Monte Carlo simulations at a single temperature, one obtains the dynamic evolution of physical quantities at different temperatures. But it is somewhat unsatisfactory that for the method suggested in Ref. [48], the reweighting temperatures need to be fixed before simulations, and one pays extra computer time in proportion to the number of reweighting temperatures.

The purpose of this article is to study numerically the effect of quenched bond randomness on the softening of the first-order phase transition. Combining the short-time dynamic approach and dynamic reweighting techniques, we perform extensive Monte Carlo simulations for the 3D random-bond Potts model and provide an estimate of the tricritical point and critical exponents of the induced continuous phase transition. On the other hand, we aim at some improvement of the dynamic reweighting method and apply the method to more complex systems. The short-time dynamic approach to the weak first-order phase transition is also attractive in this context.

The models, the dynamic scaling analysis, and an improved nonequilibrium reweighting method are described in Sec. II. Numerical simulations are presented in Sec. III. The final section contains the conclusions.

II. MODEL AND METHOD

A. Random-bond Potts model

The Hamiltonian of the three-dimensional q-state Potts model with quenched random interactions can be written as

$$-\frac{1}{k_B T}H=\sum_{\langle i,j\rangle}K_{ij}\delta_{\sigma_i,\sigma_j},\quad K_{ij}>0, \tag{1}$$

where the spin σ takes the values $1,\ldots,q$, $\delta_{\sigma_i,\sigma_j}$ is the Kronecker delta function, and the sum is over nearest-neighbor pairs on a cubic lattice. The dimensionless couplings K_{ij} are selected from two positive values of $K_1=K$ and $K_2=rK$, with a strong to weak coupling ratio $r=K_2/K_1$ called the *disorder amplitude*, according to a bimodal distribution,

$$P(K_{ij})=p\,\delta(K_{ij}-K_1)+(1-p)\,\delta(K_{ij}-K_2). \tag{2}$$

The case of $r=1$ corresponds to the pure Potts model.

In this paper, we study the case of $q=3$, $p=0.5$ (a symmetric distribution) with a combination of the short-time dynamic approach and reweighting techniques. Monte Carlo simulations with a standard Metropolis algorithm are performed on a three-dimensional lattice with periodic boundary conditions. For a review of the short-time critical dynamics and its applications, see Refs. [33,39].

The physical observables we measure are the time-dependent magnetization, its second moment, and the autocorrelation function of the q-state Potts model respectively defined as

$$M(t)=\frac{q}{(q-1)L^3}\left\langle\sum_i\left(\delta_{\sigma_i(t),1}-\frac{1}{q}\right)\right\rangle, \tag{3}$$

$$M^{(2)}(t)=\frac{q^2}{(q-1)^2L^6}\left\langle\left[\sum_i\left(\delta_{\sigma_i(t),1}-\frac{1}{q}\right)\right]^2\right\rangle, \tag{4}$$

$$A(t)=\frac{q}{(q-1)L^3}\left\langle\sum_i\left(\delta_{\sigma_i(0),\sigma_i(t)}-\frac{1}{q}\right)\right\rangle, \tag{5}$$

where L is the lattice size.

B. Nonequilibrium reweighting method

Ferrenberg and Swendsen [42] first introduced the histogram reweighting method to calculate statistical properties of a system in equilibrium. The thermal averages for a range of temperatures can be obtained from simulations at a single temperature. Then the multihistogram algorithm was proposed [43] to increase the effective reweighting range and minimize the statistical errors. A great improvement was achieved when artificial ensembles were applied to the reweighting mehtods [44,46]. Instead of the canonical distribution of the energy histogram, a "flat" histogram was obtained. Recently, Wang and Landau [45] presented a simple method to obtain the flat histogram. These reweighting techniques have greatly improved the efficiencies of Monte Carlo simulations in equilibrium.

Very recently, a reweighting method applicable to nonequlibrium Markov processes was reported [48]. Consider a simulation up to the tth Monte Carlo step as a sequence of states,

$$\vec{x}_t=(\sigma_1,\sigma_2,\ldots,\sigma_t) \tag{6}$$

where σ_t is the spin configuration of the system at time t. Hereafter, we refer to the Monte Carlo step simply as the time of simulation. At an inverse temperature $\beta=1/k_{\mathrm{B}}T$, the dynamical thermal average of an observable $O(t)$ can be obtained by $\langle O(t)\rangle_\beta=(1/n)\Sigma_{j=1}^{n}O(\sigma_t^j)$, where σ_t^j are the spin configurations from $\{\vec{x}_t^j,j=1,\ldots,n\}$, a set of paths obtained in the simulations at a fixed β. To calculate the dynamical thermal average at another temperature β', the measured observable $O(\sigma_t^j)$ has to be reweighted with a set of weights $\{w_t^j\}$. For the same set of paths $\{\vec{x}_t^j\}$, the thermal average at β' is obtained as

$$\langle O(t)\rangle_{\beta'}=\sum_{j=1}^{n}w_t^jO(\sigma_t^j)\Bigg/\sum_{j=1}^{n}w_t^j. \tag{7}$$

Here the weights w_t^j can be obtained by

$$w_{t+1}^j = \frac{P_{\beta'}(\sigma_{t+1}^j|\sigma_t^j)}{P_\beta(\sigma_{t+1}^j|\sigma_t^j)} w_t^j \quad \text{with } w_1^j = 1, \tag{8}$$

where $P(\sigma_{t+1}^j|\sigma_t^j)$ is the transition probability of the Monte Carlo algorithm.

However, if the weights are directly updated in the algorithm as in Ref. [48], one needs to predetermine the reweighting temperatures. The more temperatures we intend to reweight, the more computer time it will take in the simulation. Especially, in some cases one is not sure which temperatures are needed before the simulations. To improve the algorithm, we propose the following algorithm for each path $\vec{x}_t^j, j=1,\ldots,n$, to calculate the weights.

(1) Choose a spin and flip it according to the Metroplolis algorithm, with a transition probability $P_\beta(\sigma'^j|\sigma_t^j) = \min[1, \exp(-\beta\Delta E)]$. Here, ΔE is the energy change due to the trial spin flip from σ_t^j to σ'^j.

(2) At this point, there are three possible outcomes.

(a) If $\Delta E \leqslant 0$, the trial spin flip is always accepted and we need do nothing.

(b) If $\Delta E > 0$ and the trial spin flip is accepted, we add 1 to $n_b^j(\Delta E, t)$.

(c) If $\Delta E > 0$ and the trial spin flip is rejected, we add 1 to $n_c^j(\Delta E, t)$.

Here, $n^j(\Delta E, t)$ is a function to count the number of a certain energy change ΔE up to time t in the path j. $n^j(\Delta E, t)$ should be updated in every spin flip, but recorded only at the time steps when the measurements are performed.

Obviously, the set of weights w_t^j depend on the simulation temperature β, the new temperature β', and the energy change ΔE, but not on the concrete spin configuration. We can restore different sets of weights at different temperatures from the same set of ΔE by

$$w_t^j = \prod_{\Delta E} \exp[-(\beta' - \beta) n_b^j(\Delta E, t) \Delta E] \times \prod_{\Delta E} \left[\frac{1 - \exp(-\beta' \Delta E)}{1 - \exp(-\beta \Delta E)} \right]^{n_c^j(\Delta E, t)}, \tag{9}$$

where the product is over all possible energy change ΔE due to the spin flip. In fact, the first term can be written as $\exp[-(\beta' - \beta) E_b^j(t)]$. Here, $E_b^j(t)$ is to record the sum of the energy change in case b of step 2 up to time t. For the nearest interaction, the number of ΔE is very small. In the case of the 3D random-bond Potts model, there are 28 kinds of positive energy change when a spin is flipped ($r \neq 1$). Using this algorithm, we add nearly no extra computer time to a single simulation and, in principle, can reweight the observables to any temperatures that need not to be predetermined.

C. Dynamic scaling analysis

In the last decade, it has been discovered that already in a macroscopic *short-time* regime the universal scaling behavior emerges. The physical origin of the scaling behavior is the divergent correlating time of the second-order phase transition. A dynamic scaling form, which is valid up to the macroscopic short-time regime, has been derived with an ϵ expansion up to two-loop order by Janssen *et al.* [29,33], and its finite-size form—e.g., for the kth moment of the magnetization—is written as

$$M^{(k)}(t, \tau, L, m_0) = b^{-k\beta/\nu} M^{(k)}(b^{-z}t, b^{1/\nu}\tau, b^{-1}L, b^{x_0} m_0). \tag{10}$$

Here b is a rescaling factor, τ is the reduced temperature, β and ν are the static critical exponents, and z is the dynamic exponent, while the new independent exponent x_0 is the scaling dimension of the initial magnetization m_0, and m_0 is assumed to be small, around the fixed point $m_0 = 0$. It is important that from the scaling behavior of Eq. (10) it is possible to extract not only the dynamic exponents x_0 and z but also the static exponents originally defined in equilibrium. Since the nonequilibrium spatial correlation length at the early stage of the time evolution is small, the finite-size effect can be easily controlled. Measurements now are carried out at an early stage of the time evolution; therefore, one does not suffer from a critical slowing down.

In general, for the determination of the dynamic exponent z and static exponents, a dynamic process starting from a completely *ordered* state is more favorable, since there is less fluctuation. In this case, the dynamic system is at another fixed point $m_0 = 1$ [in contrast to the fixed point $m_0 = 0$ relevant for Eq. (10)]. The scaling variable m_0 now becomes irrelevant for the dynamic scaling behavior, and it can be simply removed from Eq. (10) [33]. Assuming that the lattice is sufficiently large, the dynamic scaling form of the magnetization around the critical point is written as

$$M(t, \tau) = t^{-c_1} F(t^{1/\nu z}\tau), \quad c_1 = \beta/\nu z. \tag{11}$$

If $\tau = 0$, the magnetization decays by a power law $M(t) \sim t^{-c1}$. If $\tau \neq 0$, the power-law behavior is modified by the scaling function $F(t^{1/\nu z}\tau)$. From this fact, one determines the critical point and the critical exponent $\beta/\nu z$. To estimate the exponent $1/(\nu z)$, we differentiate $\ln M(t, \tau)$ and obtain

$$\partial_\tau \ln M\,(t, \tau)\big|_{\tau=0} \sim t^{c_l}, \quad c_l = 1/\nu z. \tag{12}$$

In order to measure the dynamic exponent z *independently*, we introduce a time-dependent Binder cumulant $U = M^{(2)}/M^2 - 1$, and the finite-size scaling analysis shows

$$U(t, L) \sim t^{c_2}, \quad c_2 = d/z. \tag{13}$$

For a magnetic system which is initially in a high-temperature state, suddenly quenched to the critical temperature T_c and then released for the dynamic evolution, two interesting observables are the second moment of the magnetization and the autocorrelation function. For $\tau = 0$ and $m_0 = 0$, it is well known [30,33] that

$$M^{(2)}(t) \sim t^y, \quad y = (d - 2\beta/\nu)/z. \tag{14}$$

Careful analysis [49] reveals that the autocorrelation function behaves like

$$A(t) \sim t^{-\lambda}, \quad \lambda = \frac{d}{z} - \frac{x_0 - \beta/\nu}{z}. \tag{15}$$

Interesting here is that even though $m_0 = 0$, the exponent x_0

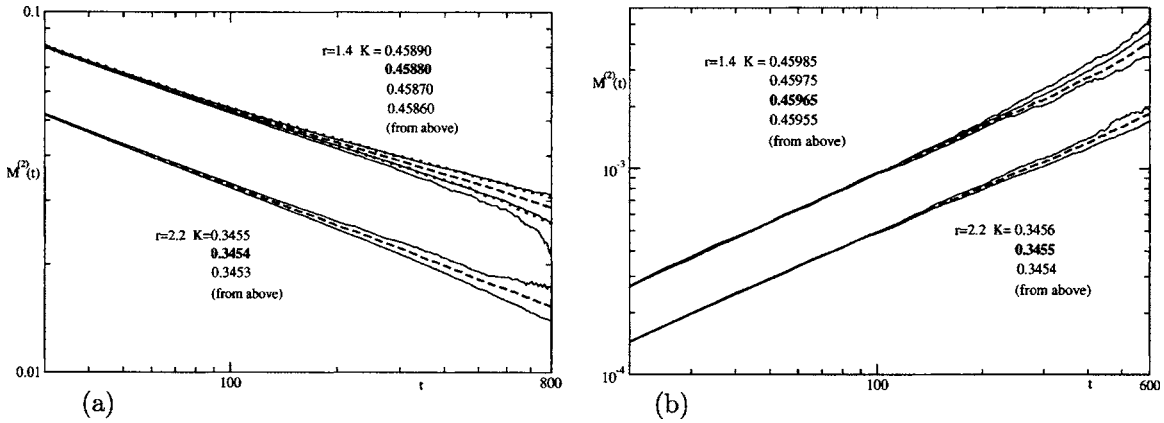

FIG. 1. The second moment obtained with the dynamic reweighting method for $r=1.4$ and $r=2.2$ and with a lattice size $L=40$ plotted vs t on a log-log scale: (a) $M^{(2)}(t)$ with an ordered start from simulations at a single temperature $K=0.4588$ for $r=1.4$ and $K=0.34535$ for $r=2.2$, respectively. The bold dashed line is the closest to the pseudocritical point K^{**}. For comparison, two other direct simulations at temperatures $K=0.4589$ and 0.4587 are displayed with dotted lines. (b) $M^{(2)}(t)$ with a disordered start from simulations at a single temperature $K=0.4597$ for $r=1.4$ and $K=0.34545$ for $r=2.2$, respectively. The bold dashed line is the closest to the pseudocritical point K^{*}.

still enters the autocorrelation function. This behavior has been confirmed in a variety of statistical systems [30,33].

D. Dynamic criterion for weak first-order phase transitions

At the second-order transition temperature T_c, the short-time behavior of physical observables obeys a power law in dynamic processes starting from both a random and an ordered state. Away from T_c, the power-law behavior is modified by a scaling function [33]. If the phase transition is of first order, independent of the initial states, physical observables at the transition temperature do not present a power-law behavior due to the finite correlating time and/or the symmetry breaking.

Around a first-order transition point, it is well known that for $K>K_c$ there is a disordered metastable state, which vanishes at a certain K^*. For $K<K_c$ there exists an ordered metastable state, which disappears at K^{**}. For a weak first-order phase transition, both K^* and K^{**} look like critical points if the system remains in the disordered and ordered metastable states, respectively. K^* and K^{**} are named pseudocritical points.

In equilibrium, numerical measurements of K^* and K^{**} are not easy due to finite-size effects. However, in the short-time dynamics, K^* and K^{**} can be determined rather confidently. Starting from a high-temperature state, the system at $K>K_c$ reaches the disordered metastable state first. Due to the large correlating time induced by the large spatial correlation length in the metastable state, physical observables at K^* present an approximate power-law behavior. The weaker the transition is, the cleaner the power-law behavior will be. This gives an estimate of K^*. Starting from a zero-temperature state, the system at $K<K_c$ reaches the ordered metastable state first and one can determine K^{**}. At a second-order phase transition, K^* and K^{**} overlap with the transition point K_c. Therefore, as Schülke and Zheng argued [50], the difference of K^* an K^{**} gives a criterion for a weak first-order transition. This method has been successfully applied to a couple of physical systems [51,52].

III. NUMERICAL SIMULATIONS

We have performed Monte Carlo simulations with the standard Metropolis algorithm. The maximum updating time is taken to be from 500 to 1100 Monte Carlo time steps, depending on the strength of disorder and the initial conditions. The results are presented with a lattice size $L=40$. To investigate the finite-size effect and further confirm our results, some simulations have been performed for $L=64$ and 96. Samples of the disordered couplings $\{K_{ij}\}$ for averaging are mostly from 5000 for the ordered start to 20 000 for the disordered start. For the case of strong disorder ($r=10$), 30 000 samples are collected with the ordered start for estimating the exponent $1/\nu$.

To estimate the errors, total samples are divided into three or four subgroups. Statistical errors are then calculated from independent measurements of these subgroups of samples. In addition, results of the measurements may fluctuate also for different time windows $[t_1,t_2]$ in which the measurements are performed. These errors will be taken into account if they are comparable to statistical errors. In some cases, corrections to scaling are considered when it is necessary.

A. Phase diagram and tricriticality

For the pure 3D three-state Potts model, the first-order phase transition is not so strong and the recent result [53] of the critical point is given at $K_c=0.550\,565(10)$. Combining the short-time dynamic approach and reweighting method, we estimate $K^*=0.551\,24(3)$ and $K^{**}=0.549\,75(5)$ from the time evolution of the second moment. The clear difference indicates that the phase transition is of first order. Since the crossover effect is somewhat strong when the disorder amplitude r is close to 1 (the pure case), we begin our simulations from $r=1.4$ to measure $M(t)$ and $M^{(2)}(t)$ with the ordered ($m_0=1$) and disordered ($m_0\sim 0$) initial states.

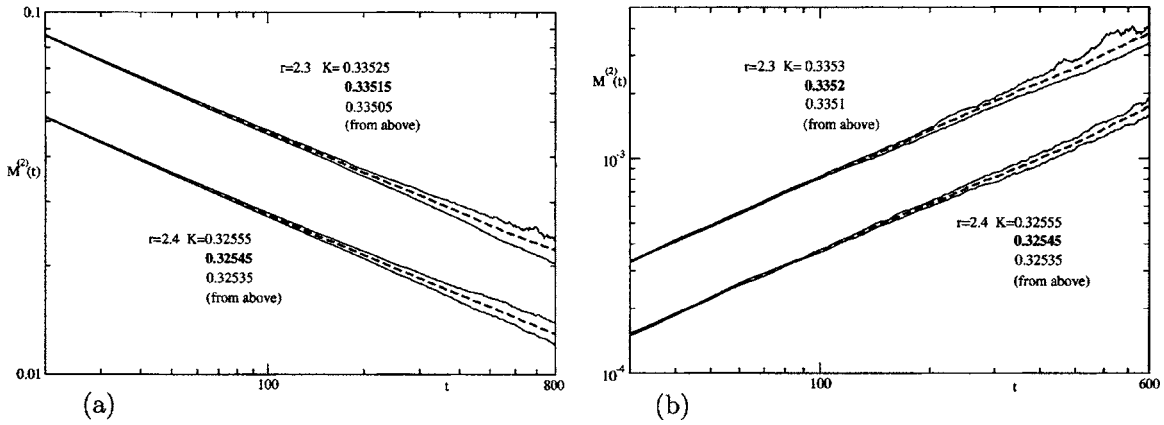

FIG. 2. The second moment obtained with the dynamic reweighting method for $r=2.3$ and $r=2.4$ and with a lattice size $L=40$ plotted vs t on a log-log scale: (a) $M^{(2)}(t)$ with an ordered start from simulations at a single temperature $K=0.3351$ for $r=2.3$ and $K=0.32545$ for $r=2.4$, respectively. The bold dashed line is the closest to the pseudocritical point K^{**}. (b) $M^{(2)}(t)$ with a disordered start from simulations at a single temperature $K=0.33515$ for $r=2.3$ and $K=0.32545$ for $r=2.4$, respectively. The bold dashed line is the closest to the pseudocritical point K^{*}.

In Fig. 1(a), the second moment with an ordered initial state is obtained from simulations at $K=0.4588$ and then reweighted to a couple of temperatures around it; averages were taken over 5000 samples. The curve exhibits a power-law-like behavior at $K^{**}=0.458\,78(7)$. In order to further confirm the reweighting approach, we have performed simulations at $K=0.4589$ and 0.4587 and compared them with the reweighting data from the simulation at $K=0.4588$. This is also shown in Fig. 1(a) with dotted lines, which fit to the corresponding solid lines within fluctuation. In Fig. 1(b), the simulation is performed at $K=0.4597$ with a disordered start and $K^{*}=0.4596(1)$ is estimated from $M^{(2)}(t)$. Similar to the case of the pure Potts model, $K^{**}<K^{*}$ detects a first-order phase transition.

For a weak first-order phase transition, the transition point K_c can be estimated from $(K^{*}+K^{**})/2$ [50]. For the 3D pure three-state Potts model, $(K^{*}+K^{**})/2=0.550\,50(6)$ is already rather close to $K=0.550\,565(10)$ from the direct measurement. The weaker the first-order phase transition is, the more accurate the estimate of K_c from $(K^{*}+K^{**})/2$ will be. At $r=1.4$, the first-order phase transition is obviously weaker than that of the pure case, since the difference $K^{*}-K^{**}$ is smaller and the second moment presents a better power-law behavior. Therefore, we expect that $(K^{*}+K^{**})/2=0.459\,20(14)$ is a relatively good estimate of the first-order phase transition point K_c, at least within the statistical errors.

We gradually increase the disorder amplitude from $r=1.4$ to 2.5. The results of $r=2.2$, 2.3, and 2.4 are displayed in Figs. 1 and 2. Carefully analyzing the data from the simulations, we find K^{*} and K^{**} at each r. The values of the pseudocritical points are summarized in Table I, and the phase diagram in the disorder-temperature plane is plotted in Fig. 3.

In Table I, we observe that the difference $\Delta K=K^{*}-K^{**}$, which measures the strength of the first-order phase transition, decreases gradually as r increases. At $r=2.2$, one can still distinguish the two pseudocritical points. At $r=2.3$, however, ΔK is so small that K^{*} and K^{**} overlap within the error bars. When $r\geqslant 2.4$, the phase transition is rounding to a continuous one. Clearly, there exists a tricritical point between $r=2.2$ and 2.4—i.e., $r_c=2.3(1)$. This result can be compared to that of the three-state bond-diluted Potts model [24], where the tricritical point in the term of the bond concentration was estimated to be 0.76(8) and the simulations were performed on a lattice size $L=16$. Our dynamic approach shows its advantage in the numerical simulations of weak first-order phase transitions.

B. Critical exponents of the continuous phase transition

Since there are rather strong corrections to scaling around the tricritical point, we choose a disorder amplitude $r=10$ for the study of the critical properties of the induced second-order transitions. In this case, however, simulations at a single temperature are not sufficient to determine the critical temperature and all the critical exponents. The fluctuations of the reweighting data are stronger due to a big disorder amplitude r. (If one reweights K_1 to $K_1+\delta K$, then, correspondingly, K_2 to $K_2+r\delta K$.) Therefore, we perform simulations at three separate temperatures for each dynamic process. In Fig.

TABLE I. Pseudocritical points K^{**} and K^{*} with different disorder amplitude r, measured with the short-time dynamic approach and the nonequilibrium reweighting method for the 3D three-state random-bond Potts model. The tricritical point is estimated to be $r_c=2.3(1)$.

	$r=1.4$	$r=1.6$	$r=1.8$	$r=2$	$r=2.2$	$r=2.3$	$r=2.4$	$r=2.5$
K^{**}	0.45878(7)	0.42386(4)	0.39403(11)	0.36805(8)	0.34541(5)	0.33514(6)	0.32544(6)	0.31626(4)
K^{*}	0.45962(12)	0.42455(5)	0.39442(9)	0.36843(7)	0.34553(6)	0.33521(7)	0.32545(5)	0.31625(5)

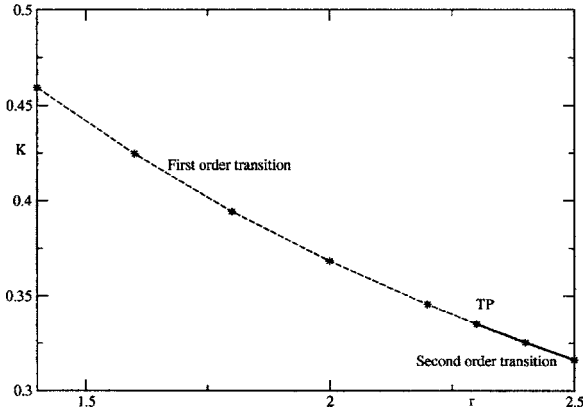

FIG. 3. Phase diagram of the 3D three-state random bond Potts model. The dashed line is the transition, line of the first-order phase transition, and the solid line is that of the second-order phase transition. The tricritical point (TP) is around $r_c=2.3(1)$.

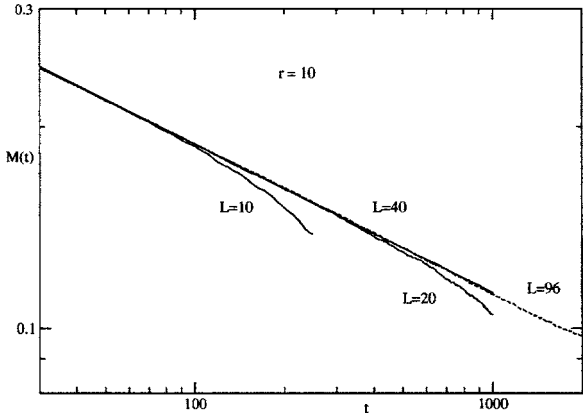

FIG. 5. The magnetization with an ordered start for $r=10$ at $K_c=0.10265$ plotted vs t on a log-log scale. The solid lines are for a lattice size $L=10$, 20, and 40, respectively. The dashed line is for a lattice size $L=96$ to a maximum time $t=2000$.

4, we determine the critical point $K_c=0.102\,65(5)$ with data in a time interval $[t_1,t_2]=[40,1000]$. The error given here includes the statistical error (obtained by dividing the samples into subgroups) and the fluctuation in the time direction. For example, for the dynamic relaxation from an ordered state, we obtain $K_c=0.102\,65$ with a statistical error 0.000 02, while the value of K_c increases slightly when t_1 changes from $t_1=10$ to $t_1=100$ and the variation is about 0.000 04. Taking into account also the dynamic relaxation from a disordered state, we come to $K_c=0.102\,65(5)$.

In Fig. 5, the curve of $M(t)$ at K_c starting from the ordered initial state with a lattice size $L=40$ is displayed on a double-logarithmic scale. It exhibits a perfect power-law behavior in Eq. (11). Thus the exponent $\beta/\nu z$ can be estimated from the slope of the curve. In order to study the possible finite-size effect and further confirm our results, some simulations at the same temperature have been performed with lattice sizes $L=10$, 20, and 96 up to a maximum updating time of 250, 1000, and 2000, respectively. Obviously, within 1000 time steps, the curves of $L=40$ and 96 overlap each other within fluctuations, indicating negligible finite-size effects.

To extract the dynamic exponent z independently, we examine the dynamic behavior of the time-dependent Binder cumulant. Because of the crossover effect, corrections to scaling of the Binder cumulant are detected in the early times. Therefore, we fit the curve to the form of $U(t) \sim t^{d/z}(1+c/t^b)$. (In Ref. [24], corrections to scaling are also considered to extract the critical exponents.) In Fig. 6(a), a good fit of $U(t)$ is clearly seen in a time interval [10, 1000], and the dynamic exponent is estimated to be $z=2.47(5)$. If corrections to scaling are not taken into account, a direct power-law fit yields a dynamic exponent z about 5% smaller. Taking the dynamic exponent z as input, we can calculate the critical exponent β/ν from $\beta/\nu z$ measured in Fig. 5.

From the data of the magnetization in the neighborhood of K_c, we can approximately calculate the differentiation $\ln M(t,\tau)$ and then estimate the exponent $1/\nu z$ according to Eq. (12). For this purpose, we perform simulations at K_c (or a K very close to K_c) and other two K's about half percent away from K_c, and then calculate $\ln M(t,\tau)$ with quadratical approximations. Here we observe also corrections to scaling and therefore fit the data to $\partial_\tau \ln M(t,\tau)|_{\tau=0} \sim t^{1/\nu z}(1+c/t^b)$.

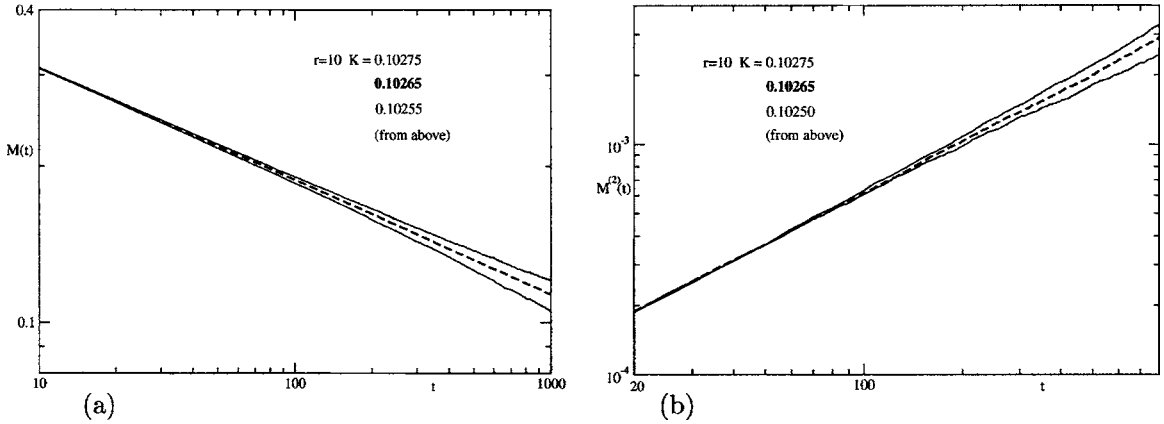

FIG. 4. The magnetization and second moment for $r=10$ and with a lattice size $L=40$ plotted vs t on a log-log scale: (a) $M(t)$ with an ordered start from simulations at temperatures $K=0.10275$, 0.10265, and 0.10255. The bold dashed line is the closest to the critical point K^{**}. (b) $M^{(2)}(t)$ with a disordered start from simulations at temperatures $K=0.10275$, 0.10265, and 0.10250. The bold dashed line is the closest to the critical point K^*.

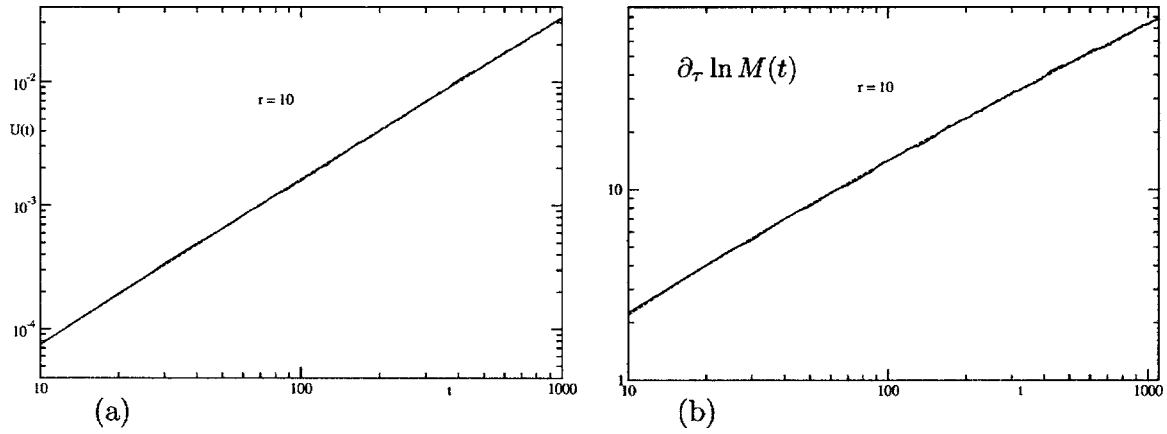

FIG. 6. The Binder cumulant and $\partial_\tau \ln M(t)$ with an ordered start for $r=10$ at $K_c=0.10265$ plotted vs t on a log-log scale: (a) $U(t)$ is plotted with a solid line. The dashed line shows a fit with corrections to scaling. (b) $\partial_\tau \ln M(t)$ is plotted with a solid line. The dashed line shows a fit with corrections to scaling.

This is shown in Fig. 6(b), and a nice fit is observed in a time interval from $t=10$ to 1100. The exponent $1/\nu z$ is estimated to be 0.573(16). Thus we obtain the exponent $1/\nu=1.42(7)$ with z as an input. Since the corrections to scaling here are relatively strong, a simple power-law fit would yield an exponent $1/\nu z$ about 20% bigger. Therefore, the corrections to scaling are essential here to keep the value of $1/\nu$ within the upper bound $d/2$ [54].

Here the correction exponent b is small for both the time-dependent Binder cumulant and $\ln M(t,\tau)$, and the fittings give $b=0.017$ with $c=-0.935$ and 0.026 with $c=-0.982$ for the Binder cumulant and $\ln M(t,\tau)$, respectively. Therefore, it is possible to fit the curves with logarithmic corrections. The exponents are estimated to be $z=2.50(3)$ and $1/\nu=1.40(6)$, well consistent with $z=2.47(5)$ and $1/\nu=1.42(7)$ from the power-law corrections. After corrections to scaling are taken into account, variations in the time direction become not so prominent, comparable to statistical errors. For the dynamic exponent z, both the statistical error and variation in the time direction are about 1%; therefore, it comes up with a total error of 2%. The situation is similar for the index $1/\nu z$.

Further, we have performed the simulations starting from a disordered initial state. In Fig. 7(a), $M^{(2)}(t)$ is plotted on a log-log scale, and a nice power-law behavior is observed. Based on Eq. (14), from the slope of the curve in a time interval [50, 1000] the exponent $y=(d-2\beta/\nu)/z$ is estimated to be $y=0.761(14)$. Simulations have been also performed at the same temperature with a lattice size=64. The curves for both $L=40$ and 64 coincide well, and it shows that the finite-size effect is negligibly small in this time regime. Another interesting observable here is the autocorrelation function, which is governed by the "new" exponent x_0. The curve is plotted in Fig. 7(b), which presents also a power-law behavior. From the slope of the curve in a time interval [5, 100], we estimate the index $\lambda=d/z-(x_0-\beta/\nu)/z=1.19(1)$ in Eq. (15). The fluctuation beyond $t=100$ is very large.

Finally, we find that corrections to scaling are negligibly small in a dynamic relaxation from a disordered state (such a phenomenon is also reported in the literature [55]). If one fits the curves in Fig. 7 with a power-law correction—e.g., $M^{(2)}(t)\sim t^y(1+c/t^b)$—one finds a nearly zero parameter c in the small-b regime (or for a logarithmic correction), and the index y is almost unchanged. In the large-b regime, no stable

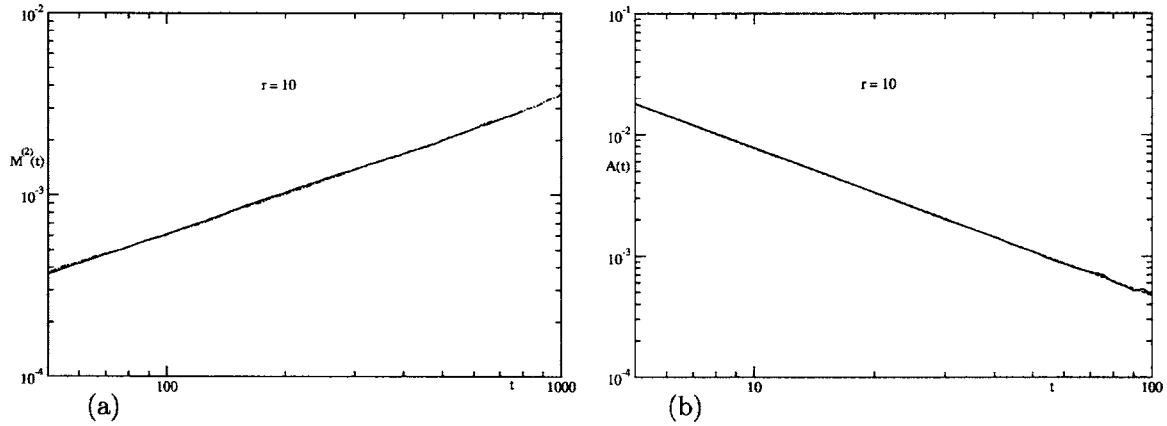

FIG. 7. The second moment and autocorrelation with an disorder start for $r=10$ at $K_c=0.10265$ plotted vs t on a log-log scale: (a) $M^{(2)}(t)$ is plotted with a solid line. The dashed line is for a lattice size $L=64$ to a maximum time $t=1000$. (b) $A(t)$ is plotted with a solid line. The dashed line shows a power-law fit.

TABLE II. The critical exponents for the 3D three-state random-bond Potts (RBP) model with $r=10$, measured from $A(t)$, $M^{(2)}(t)$, $M(t)$, $\partial_\tau \ln M(t,\tau)$, and $U(t)$, respectively, starting from both the random and ordered initial states.

	m_0	RBP
$y=(d-2\beta/\nu)/z$	0.0	0.761(14)
λ		1.19(1)
$c_1=\beta/\nu z$	1.0	0.221(1)
$c_2=d/z$		1.216(14)
$c_l=1/\nu z$		0.573(16)
$z=d/c_2$		2.47(5)
$z=d/(y+2c_1)$		2.49(5)
$\beta/\nu=zc_1$		0.548(13)
$1/\nu=zc_l$		1.42(7)

fit is observed. Therefore, errors of the indices y and λ are mainly statistical errors.

In Table II, all our measurements of the critical exponents of the three-dimensional three-state random-bond Potts model are summarized. For the dynamic exponent z, one estimates its value either from $z=d/c_2=2.47(5)$ or from $z=d/(y+2c_1)=2.49(5)$. These two values agree well within statistical errors and support the dynamic approach to the disordered Potts model. The static exponents β/ν and $1/\nu$ are calculated with an average $z=2.48(5)$.

For comparison, the critical exponents are listed in Table III for the three-dimensional three-state site-diluted Ising model, the three-state site-diluted, four-state bond-diluted Potts, and large-q-state random-bond Potts models. Within statistical errors, our value $1/\nu=1.42(7)$ is consistent with $1/\nu=1.449(11)$ for the three-state site-diluted Potts model [23]. This supports the universality of phase transitions with respect to the form of (strong) disorder. We also observe that the static exponents of the random-bond Potts model are relatively close to those of the site-diluted Ising model and also the large-q-state random-bond Potts model.

TABLE III. The critical exponents for the 3D three-state random-bond Potts (RBP) model, site-diluted Ising (SDI) model [27], three-state site-diluted Potts (SDP) model [23], four-state bond-diluted Potts (BDP) model [24], and large q-state random-bond Potts (LRBP) model [28].

	RBP	SDI	SDP	BDP	LRBP
$1/\nu$	1.42(7)	1.462(11)	1.449(11)	1.330(25)	1.37(2)
β/ν	0.548(13)	0.519(8)		0.65(5)	0.60(2)
z	2.48(5)				
λ	1.19(1)				

IV. CONCLUSION

With extensive dynamic Monte Carlo simulations, we have investigated the effect of bond randomness on the rounding of the phase transitions of the 3D random-bond Potts model. We obtain the phase diagram in the weakly disordered regime and give an estimate of the tricritical point $r_c=2.3(1)$. At a strong disorder amplitude $r=10$, we study the critical properties of the induced continuous transition. We make an attempt to improve the recently suggested non-equilibrium reweighting method and apply it to the short-time dynamic Monte Carlo simulations of second-order and weak first-order phase transitions. The dynamic approach shows its merit in estimating the pseudocritical points K^* and K^{**} around a weak first-order phase transition and in tackling the dynamic and static properties of disordered systems.

ACKNOWLEDGMENTS

The authors would like to thank A. P. Young and W. Janke for helpful discussions. This work was supported in part by NNSF China under Grant Nos. 10325520 and 10275054, SRFDP (China), and DFG (Germany) under Grant No. TR 300/3-4.

[1] L. Schwenger, K. Budde, C. Voges, and H. Pfnür, Phys. Rev. Lett. **73**, 296 (1994).
[2] G. S. Iannacchione, G. P. Crawford, S. Zumer, J. W. Doane, and D. Finotello, Phys. Rev. Lett. **71**, 2595 (1993).
[3] Y. Imry and M. Wortis, Phys. Rev. B **19**, 3580 (1979).
[4] K. Hui and A. N. Berker, Phys. Rev. Lett. **62**, 2507 (1989).
[5] M. Aizenman and J. Wehr, Phys. Rev. Lett. **62**, 2503 (1989).
[6] W. Kinzel and E. Domany, Phys. Rev. B **23**, 3421 (1981).
[7] A. W. W. Ludwig, Nucl. Phys. B **330**, 639 (1990).
[8] S. Chen, A. M. Ferrenberg, and D. P. Landau, Phys. Rev. Lett. **69**, 1213 (1992).
[9] S. Chen, A. M. Ferrenberg, and D. P. Landau, Phys. Rev. E **52**, 1377 (1995).
[10] V. Dotsenko, M. Picco, and P. Pujol, Nucl. Phys. B **455**, 701 (1995).
[11] M. Picco, Phys. Rev. B **54**, 14930 (1996).
[12] J. Cardy and J. L. Jacobsen, Phys. Rev. Lett. **79**, 4063 (1997).
[13] C. Chatelain and B. Berche, Phys. Rev. Lett. **80**, 1670 (1998).
[14] J. L. Jacobsen and J. Cardy, Nucl. Phys. B **515**, 701 (1998).
[15] F. Yasar, Y. Gündüc, and T. Celik, Phys. Rev. E **58**, 4210 (1998).
[16] Ricardo Paredes V. and J. Valbuena, Phys. Rev. E **59**, 6275 (1999).
[17] T. Olson and A. P. Young, Phys. Rev. B **60**, 3428 (1999).
[18] C. Chatelain and B. Berche, Nucl. Phys. B **572[FS]**, 626 (2000).
[19] C. Deroulers and A. P. Young, Phys. Rev. B **66**, 014438 (2002).
[20] J-Ch. Anglés d'Auriac and F. Iglói, Phys. Rev. Lett. **90**, 190601 (2003).
[21] J. Q. Yin, B. Zheng, and S. Trimper, Phys. Rev. E **70**, 056134 (2004).
[22] K. Uzelac, A. Hasmy, and R. Jullien, Phys. Rev. Lett. **74**, 422 (1995).

[23] H. G. Ballesteros, L. A. Fernández, V. Martín-Mayor, A. Muñoz Sudupe, G. Parisi, and J. J. Ruiz-Lorenzo, Phys. Rev. B **61**, 3215 (2000).
[24] C. Chatelain, B. Berche, W. Janke, and P. E. Berche, Phys. Rev. E **64**, 036120 (2001).
[25] J. S. Wang and D. Chowdhury, J. Phys. (France) **50**, 2905 (1989).
[26] H. O. Heuer, J. Phys. A **26**, L333 (1993).
[27] H. G. Ballesteros, L. A. Fernández, V. Martín-Mayor, A. Muñoz Sudupe, G. Parisi, and J. J. Ruiz-Lorenzo, Phys. Rev. B **58**, 2740 (1998).
[28] M. T. Mercaldo, J-Ch. Anglés d'Auriac, and F. Iglói, Europhys. Lett. **70**, 733 (2005).
[29] H. K. Janssen, B. Schaub, and B. Schmittmann, Z. Phys. B: Condens. Matter **73**, 539 (1989).
[30] D. A. Huse, Phys. Rev. B **40**, 304 (1989).
[31] K. Humayun and A. J. Bray, J. Phys. A **24**, 1915 (1991).
[32] Z. B. Li, U. Ritschel, and B. Zheng, J. Phys. A **27**, L837 (1994).
[33] B. Zheng, Int. J. Mod. Phys. B **12**, 1419 (1998), review article.
[34] B. Zheng, M. Schulz, and S. Trimper, Phys. Rev. Lett. **82**, 1891 (1999).
[35] D. Stauffer, Physica A **186**, 197 (1992).
[36] N. Ito, Physica A **196**, 591 (1993).
[37] H. J. Luo, L. Schülke, and B. Zheng, Phys. Rev. Lett. **81**, 180 (1998).
[38] N. Ito and Y. Ozeki, Physica A **321**, 262 (2003).
[39] B. Zheng, in *Computer Simulation Studies in Condensed-Matter Physics XVII*, edited by D. P. Landau (Springer, Heidelberg, 2004).
[40] B. Zheng and H. J. Luo, Phys. Rev. E **63**, 066130 (2001).
[41] Y. Ozeki and N. Ito, Phys. Rev. B **64**, 024416 (2001).
[42] A. M. Ferrenberg and R. H. Swendsen, Phys. Rev. Lett. **61**, 2635 (1988).
[43] J. S. Wang, R. H. Swendsen, and R. Kotecký, Phys. Rev. Lett. **63**, 109 (1989).
[44] T. P. P. M. C. de Oliveira and H. Herrmann, Braz. J. Phys. **26**, 677 (1996).
[45] F. Wang and D. P. Landau, Phys. Rev. Lett. **86**, 2050 (2001).
[46] J. S. Wang and R. H. Swendsen, J. Stat. Phys. **106**, 245 (2002).
[47] R. Dickman, Phys. Rev. E **60**, R2441 (1999).
[48] H. K. Lee and Y. Okabe, Phys. Rev. E **71**, 015102 (2005).
[49] H. K. Janssen, in *From Phase Transition to Chaos*, edited by G. Györgyi, I. Kondor, L. Sasvári, and T. Tél, Topics in Modern Statistical Physics (World Scientific, Singapore, 1992).
[50] L. Schülke and B. Zheng, Phys. Rev. E **62**, 7482 (2000).
[51] E. V. Albano, Phys. Lett. A **288**, 73 (2001).
[52] G. P. Saracco and E. V. Albano, J. Chem. Phys. **118**, 4157 (2003).
[53] W. Janke and R. Villanove, Nucl. Phys. B **489**[FS], 679 (1997).
[54] J. T. Chayes, L. Chayes, D. S. Fisher, and T. Spencer, Phys. Rev. Lett. **57**, 2999 (1986).
[55] G. P. Zheng and M. Li, Phys. Rev. E **65**, 036130 (2002).